

International Journal of Engineering Sciences & Research Technology

(A Peer Reviewed Online Journal)
Impact Factor: 5.164



Chief Editor
Dr. J.B. Helonde

Executive Editor
Mr. Somil Mayur Shah

INTERNATIONAL JOURNAL OF ENGINEERING SCIENCES & RESEARCH
TECHNOLOGY
CLEANED EEG SIGNAL: AUTOMATIC EEG ARTIFACT REMOVAL FOR BRAIN
MONITORING

Govind M^{*1} & Deepa T R^{2*}

Electronics & Communication, College of Engineering Karunagappally, Kerala, India

DOI: 10.5281/zenodo.2631569

ABSTRACT

An effective method for removal of noises in Electroencephalogram was developed and evaluated. This noise is called artifacts in EEG signal. The method targets most types of artifacts and works without user interaction. The method uses the neurophysiologic model of EEG signal and an iterative Bayesian estimation scheme. Artifact removal algorithm effectively removes artifacts from EEGs and improves the quality of EEG signal impaired by artifacts. Only in rare cases did the algorithm slightly attenuate EEG patterns, but the clear visibility of significant patterns was preserved. Artifact removal methods work either semi-automatically or with insufficient reliability for clinical use, whereas the clean EEG method works fully automatically and leaves true EEG patterns unchanged with a high reliability. The artifact removal algorithm removes noise with less amount of time. Here the classification of EEG bands are considered for effective monitoring of human brain.

KEYWORDS: Electroencephalogram, Artifacts, Bayesian Estimation, Neurophysiological model

1. INTRODUCTION

The electroencephalogram (EEG) is an important tool in the diagnosis of neurological disorders and the investigation of the functional properties of the brain. Unfortunately, EEG recordings are commonly contaminated by artifacts(noise), potentials that do not originate from the brain but from various other sources. Artifacts are classified into Physiological and Non-physiologic artifacts originate from various sources of electrical fields causing interference in the frequency band of EEGs. These sources include mains electricity noise at a frequency of 50 or 60 Hz, depending on the geographic region. Electric fields in external electronic devices, like mobile phones or implanted devices, like cardiac pacemakers also cause interference at frequencies relevant for EEGs. High-amplitude artifacts are often due to electromechanic machines, such as ventilators, feeding or infusion pumps or intravenous drips.

The most common artifacts are caused by a faulty electrical connection of the electrodes and the skin of the patient, which is frequently a problem in long-term recordings. Patient movements often temporarily compromise this electrode- skin connection, giving rise to complex artifacts in the EEG. A second large group of artifacts have a physiologic origin. These comprise in particular ocular artifacts due to eye blinks and eye movements, which can be recognized by their characteristic waveforms and potential distributions in the EEG or by co-registration of an electrooculogram. Temporalis and frontal is muscles are the major source of myogenic artifacts, which may completely obscure an EEG recording due to their broad frequency spectrum and high amplitudes. Artifacts with a physiological origin also include cardiac artifacts, which can be identified by their correlation with the electrocardiogram, and also artifacts due to a cranial bone defect causing the breach effect.

The major contribution of this article is a completely novel approach proposed for fully automatic artifact removal, called clean EEG. The major intention of the proposed method is to support the visual analysis of long-term EEG recordings. Clean EEG rejects numerous types of artifacts that frequently obscure long-term recordings and impede their interpretation. More precisely, it targets artifacts that do not coincide with a spatio-temporal correlation pattern of an EEG of cerebral origin, which particularly includes artifacts due to myogenic contractions, faulty electrode-to-patient connections, patient movements and most non-physiologic sources. The method works fully automatically and without any patient-individual parameter adjustments, which also makes

it well adapted as a preprocessor for all types of computational EEG analyses, such as electrical source imaging, automatic spike and seizure detection, or evoked potential analyses.

The algorithm is based on a neurophysiological signal model, which includes one term representing the clean EEG, which originates from cerebral sources only, and one term representing a wide range of artifacts. The model characterizes spatio-temporal correlations of the EEG and utilizes a Bayesian minimum mean squared error (MMSE) estimator for the separation of pure EEG components and artifactual components. An effective, iterative procedure is proposed for the critical characterization of a priori knowledge required by Bayesian estimators. In contrast to conventional frequency filtering, which operates in the spectral domain, and methods like Independent Component Analysis and Principal Component Analysis, which operate in the spatial domain, the approach separates the clean EEG and the artifacts in the spatio-spectral domain. The advantage is a high degree of freedom, which allows artifacts to be more accurately isolated and more precisely separated from the EEG, with only very low distortions of the clean EEG components.

2. RELATED WORKS

The generation of cerebral potentials is based on the intrinsic electrophysiological properties of the nervous system. Identifying the generator source and electrical field of propagation are the basis for recognizing electrographic patterns that underlay the expression of the “brain waves” as normal or abnormal. Most common EEGs recorded at the surface of the scalp represent pooled electrical activity generated by large numbers of neurons.

Electrical signals are generated when electrical charges move within the central nervous system. Neural function is maintained by ionic gradients established by neuronal membranes. Sufficient duration and length of small amounts ie, in micro Volt unit of electrical currents of cerebral activity are required to be amplified and displayed for interpretation. A resting membrane potential normally exists through the efflux of positive-charged (potassium) ions maintaining an electrochemical equilibrium of -75 mV. With depolarization, an influx of positive-charged (sodium) ions that exceeds the normal electrochemical resting state occurs. Channel opening within the lipid bilayer is through a voltage-dependent mechanism, and closure is time dependent.

Conduction to adjacent portions of the nerve cell membranes results in an action potential when the depolarization threshold is exceeded. However, it is the synaptic potentials that are the most important source of the extracellular current flow that produces potentials in the EEG. Excitatory postsynaptic potentials (EPPs) flow inwardly (extracellular to intracellular) to other parts of the cell via sodium or calcium ions. Inhibitory post-synaptic potentials (IPPs) flow outwardly (intracellular to extracellular) in the opposite direction (source), and involve chloride or potassium ions. These summed potentials are longer in duration than action potentials and are responsible for most of the EEG waveforms.

The brainstem and thalamus serve as subcortical generators to synchronize populations of neocortical neurons in both normal (i.e., sleep elements) and in abnormal situations (i.e., generalized spike-and-wave complexes). Layers of cortical neurons are the main source of the EEG. Pyramidal cells are the major contributor of the synaptic potentials that make up EEG. These neurons are arranged in a perpendicular orientation to the cortical surface from layers III, IV, and VI. Volumes large enough to allow measurement at the surface of the scalp require areas that are >6 cm², although probably >10 cm² are required for most IEDs to appear on the scalp EEG because of the attenuating properties incurred by the skull. All generators have both a positive and negative pole that function as a dipole.

Scalp EEG recording displays the difference in electrical potentials between two different sites on the head overlying cerebral cortex that is closest to the recording electrode. During frequent use, electrical potentials are acquired indirectly from the scalp surface and incorporate waveform analyses of frequency, voltage, morphology, and topography. Most of the human cortex is buried deep beneath the scalp surface, and additionally represents a two-dimensional projection of a three-dimensional source, presenting a problem for generator localization in scalp EEG. The waveforms that are recorded from the scalp represent pooled synchronous activity from large amount of neurons. That will create the cortical potentials and may not represent small interictal or ictal sources.

3. METHODS

[http:// www.ijesrt.com](http://www.ijesrt.com) © International Journal of Engineering Sciences & Research Technology

[37]



We use a set of electrodes, the recording is taken by placing the electrodes on the scalp. With the help of a conductive gel or paste, usually after preparing the scalp area by light abrasion to reduce impedance due to dead skin cells. Many systems typically use electrodes. The electrodes are attached to a wire. Some systems use caps or nets into which electrodes are embedded. This is used when high-density arrays of electrodes are needed.

Electrode locations are different. Electrode names are specified by the International 10–20 system for most clinical and research applications. The system ensures that the naming of electrodes is consistent across laboratories. In most clinical applications, 19 recording electrodes are used. A smaller number of electrodes are used when recording EEG from neonates. Additional electrodes can be added to the standard set-up when a clinical/research application demands increased spatial resolution for a particular area of the brain. High-density arrays can contain up to 256 electrodes more-or-less evenly spaced around the scalp.

Each electrode is connected to one input of a differential amplifier (one amplifier per pair of electrodes). A common system reference electrode is connected to the other input of each differential amplifier. The amplifiers amplify the voltage between the active electrode and the reference (typically 1,000–100,000 times, or 60–100 dB of voltage gain). In analog EEG, the signal is then filtered, and the EEG signal is output as the deflection of pens as paper passes underneath. Most EEG systems, are digital, and the amplified signal is digitized via an analog-to-digital converter, after being passed through an anti-aliasing filter. Analog-to-digital sampling occurs, typically at 256–512 Hz in clinical scalp EEG; sampling rates of up to 20 kHz are used in some research applications. During the recording, a chain of activation procedures may be used. These activities may induce normal or abnormal EEG activity. The procedures include hyperventilation, photic stimulation, eye closure, mental activity, sleep and sleep deprivation. During epilepsy monitoring, a patient's typical seizure medications may be withdrawn.

The digital EEG signal is stored electronically. It can be filtered for display. The value for the high-pass filter and a low-pass filter are 0.5–1 Hz and 35–70 Hz respectively. The high-pass filter filters out slow artifact, such as electrogalvanic signals and movement artefact. The low-pass filter filters out high-frequency artifacts, such as electromyographic signals. An additional band stop or notch filter is typically used to remove artifact caused by electrical power lines (60 Hz in the United States and 50 Hz in many other countries).

The EEG signals can be available with an open source hardware such as Open BCI. The signal can be processed by freely available software such as EEGLAB or the Neurophysiological Biomarker Toolbox. As part of an evaluation for epilepsy surgery, it may be necessary to insert electrodes near the surface of the brain. It is placed under the surface of the dura mater. This is called variously as Electrocorticography (ECoG), "intracranial EEG (I-EEG)" or "subdural EEG (SD-EEG)". Depth electrodes may also be placed into brain structures, such as the amygdala or hippocampus, structures, which are common epileptic foci and may not be visible clearly by scalp EEG. The electrocorticographic signal is processed in the same manner as digital scalp EEG, with a couple of caveats. ECoG is typically recorded at higher sampling rates than scalp EEG because of the requirements of Nyquist theorem the subdural signal is composed of a higher predominance of higher frequency components. Many of the artifacts that affect scalp EEG do not impact ECoG. The display filtering is often not needed.

An adult human EEG signal is in the range of 10 μ V to 100 μ V in amplitude when measured from the scalp and is about 10–20 mV when measured from subdural electrodes. Typically an EEG voltage signal represents a difference between the voltages at two electrodes. The display of the EEG for the reading encephalographer may be set up in one of several ways. The method, clean EEG, is based on a stochastic, spatio-temporal model for EEGs, which are impaired by artifacts. The model includes K channels of digital EEG recordings, represented by length- K EEG vectors $e(t)$ with discrete time indices t . The EEG vectors $e(t)$ are decomposed into a superposition of three components,

$$e(t) = e_j(t) + e_a(t) + n(t) \quad (i)$$

Where the clean EEG vectors $e_j(t)$ represent “true EEG” contributions from cerebral sources, the EEG artifact vectors $e_a(t)$ represent artifactual contributions caused by various types of artefact sources, and the noise vectors $n(t)$ contain noise due to amplification and analog-to-digital conversion and residual modeling errors. The clean

EEG artefact separation algorithm is based on a linear minimum mean square error (MMSE) estimator. This type of estimators requires a priori Knowledge of second-order moments of observations and parameters to be estimated: it seems to be an obvious assumption, that the three components pure EEG e_j , artifacts a , and noise n are uncorrelated, meaning that their covariance is zero. Furthermore, it can be assumed, due to common high-pass filters in conventional EEG recording hardware, that all components are also zero-mean.

The full characterization of second-order moments in equation (1) would include all spatial and temporal cross-correlations, given by $C_{e_j}(t, t_1)$. However, this would lead to a computationally expensive MMSE estimator that could be hardly calculated in an acceptable amount of time for commonly used sampling rates and channel numbers. A significant reduction in complexity can be achieved, if the EEG is transformed into the frequency domain denoted by $\hat{e}(v)$ and $\hat{e}(v)$. We used a discrete cosine transform, which for real-valued EEG has the advantage to be real-valued in the transform domain. Certainly, a discrete Fourier transform could also be used, which led to very similar results in our experiments.

The frequency transform can be applied in the context of the overlap-add method, such that all assumptions and approximations must be valid only within each window separately. We applied the overlap add method using Hamming windows and a distance of 1.5 seconds between succeeding frames. The linearity of allows to transform each component separately, i.e., (1) can be written in the frequency domain as $\hat{e}(v) = \hat{e}_j(v) + \hat{e}_a(v) + \hat{n}(v)$. In the frequency domain, we assume that spectral cross-correlations are approximately zero, i.e.,. For discrete cosine transforms, this assumption would be exact for 1st-order Markov processes and asymptotically exact for finite-order Markov processes. These are equivalent to processes obtained from autoregressive models, which have frequently been used in EEG signal processing methods. Due to this simplification, the statistical characterization reduces to knowledge of covariance matrices $C_{e_j}(v)$ for the pure EEG vectors, $C_{e_a}(v)$ for the EEG artifact vectors, and $C_n(v)$ for the noise vectors. The 16 channel EEG signal with artifacts is given below in Fig.1.

Characterization of the clean EEG component e_j can be based either on artefact free EEG data or on a suitable data model. Artifact free data can be cut into a sufficient number of samples and transformed into frequency domain in order to calculate, e.g., sample covariance matrices. It is possible to calculate specific covariance matrices for each individual subject, or averaged covariance matrices by mixing data samples from different subjects.

4. RESULTS

The clean EEG e_j , can be separated from artifacts e_a using a linear minimum mean square error (MMSE) estimator, which might be the most important type of Bayesian estimators. The linear MMSE estimator $e_{*j}(t)$ minimizes the mean squared error.

$$\varepsilon = E \{ \| e_{*j}(t) - e_j(t) \|^2 \} \quad (\text{ii})$$

due to the assumption of uncorrelated clean EEG e_j , artifacts a , and noise n , it can be written as,

$$e_{*j}(t) = f + (C_{e_j} C_e^{-1} e)(t) \quad (\text{iii})$$

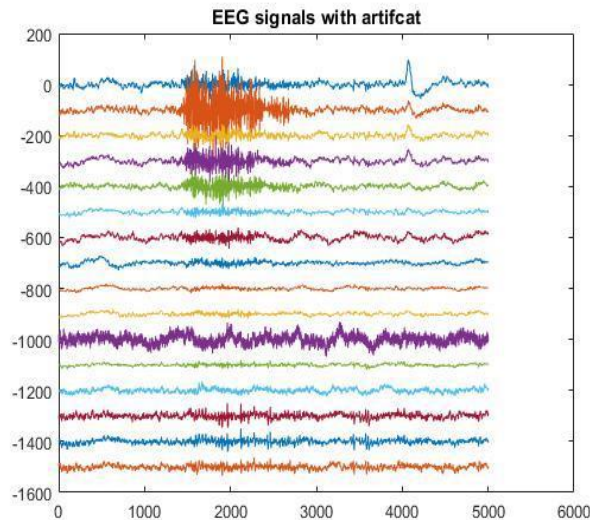


Fig.1.: EEG signal with noise/artifacts

with an inverse frequency transform denoted by $\mathcal{F}^{-1}(\cdot)$, the frequency domain EEG vector $\hat{e}(v)$ and its correlation matrix given by the sum.

$$\hat{e}(v) = \hat{e}_j(v) + M\hat{a}(v) + I \quad (\text{iv})$$

Where \hat{e}_j from equation (i) have been used. In a similarly way, a linear MMSE estimator for the artifacts a can be shown to be

$$\hat{a}(t) = \mathcal{F}^{-1}(\hat{e}(v)M^T C^{-1}) \quad (\text{v})$$

An estimator for the artefact vector ea can easily be calculated via multiplication with the montage matrix M . However, in the following subsection, we will make use of estimates for the artifact sources a directly rather than their effect on the EEG.

The mean squared error measures the average of the squares of the errors. The average squared difference between the estimated values and what is estimated. Mean square error is a risk function. It is corresponding to the expected value of the squared error loss. The mean square error is almost always strictly a positive value, not zero because of randomness or because the estimator does not account for information that could produce a more accurate estimate. The mean square error is a measure of the quality of an estimator. It is always nonnegative, and values closer to zero are better.

The mean squared error is the second order moment of the error. It incorporates both the variance of the estimator and its bias. For an unbiased estimator, the mean squared error is the variance of the estimator. Like the variance, mean squared error has the same units of measurement as the square of the quantity being estimated. In an analogy to standard deviation, taking the square root of mean square error yields the root mean square error (RMSE) or root mean square deviation (RMSD), which has the same units as the quantity being estimated; for an unbiased estimator, the root mean square is the square root of the variance, known as the standard error.

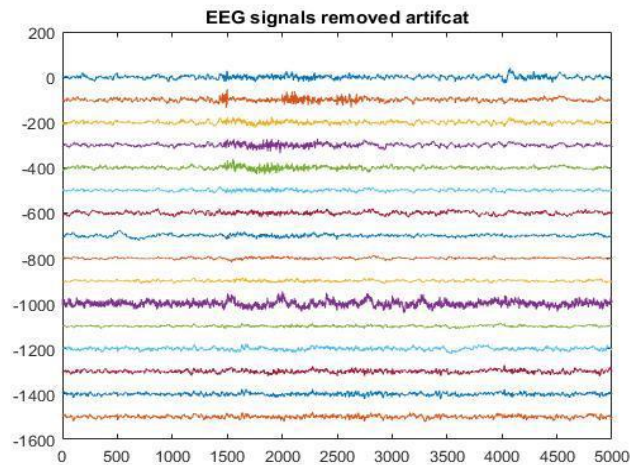


Fig.2.: EEG Signal without Artifacts

The Electroencephalogram is described in terms of rhythmic activity and transient activity. The rhythmic activity is divided into certain frequency bands. These frequency bands are a matter of nomenclature. For example, any rhythmic activity between 8–12 Hz can be described as "alpha". The designations arose because rhythmic activity within a certain frequency range was noted to have a certain distribution over the scalp or a certain biological significance. Frequency bands are usually extracted using spectral methods as implemented for instance in freely available EEG software such as EEGLAB or the Neurophysiological Biomarker Toolbox. Computational processing of the EEG is often named Electroencephalography.

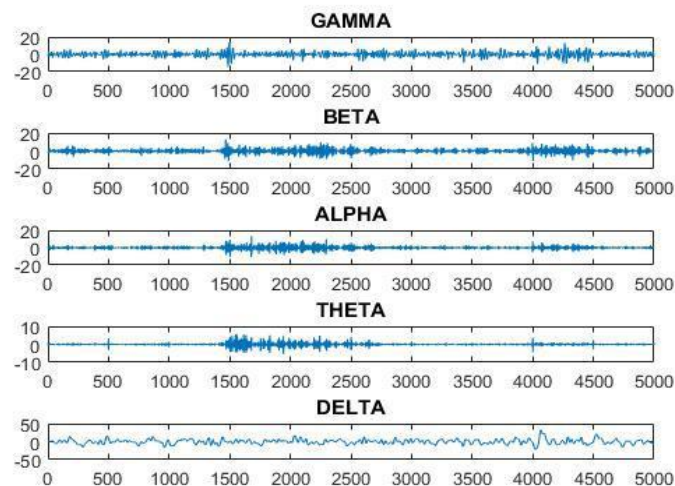


Fig.3.: EEG Frequency bands

Most of the cerebral signal observed in the scalp EEG falls in the range of 1–20 Hz (activity below or above this range is likely to be artifactual, under standard clinical recording techniques). EEG waveforms are subdivided into mainly 4 bandwidths known as alpha, beta, theta and delta to signify the majority of the EEG used in clinical practice.

5. CONCLUSIONS

The clean EEG artifact removal algorithm effectively removes artifacts from EEGs and improves the readability of EEGs impaired by artifacts. Clean EEG is a valuable tool for EEG artifact removal, which reliably preserves significant EEG patterns from cerebral sources and removes numerous types of artifacts, including myogenic artifacts, electrode artifacts, movement artifacts or line noise. A computationally efficient implementation of the algorithm makes it a viable alternative or extension to commonly used post hoc frequency filtering in EEG review software, also effectively plotted the different frequency bands of clean EEG signal and compared the performance. The method is very useful for medicinal purposes to monitor the functionality of human brain. The method is very efficient in all category irrespective of the age.

REFERENCES

- [1] M.M. Hartmann, K.Schindlerb, T.A.Gebbinkc, G.Gritscha, T.Klugea, Pure EEG:Automatic EEG artifact removal for epilepsy monitoring.
- [2] Lagerlund TD, Sharbrough FW, Busacker NE. Spatial filtering of multichannel electroencephalographic recordings through principal component analysis by singular value decomposition. *J Clin Neurophysiol Off Publ Am Electroencephalogr Soc* 1997;14(1):73—82.
- [3] Kay S. Fundamentals of statistical signal processing, volume I: estimation theory. Prentice Hall; 1993 [1. Aufl.].
- [4] Boudet S, Peyrodie L, Forzy G, Pinti A, Toumi H, Gallois P. Improvements of adaptive filtering by optimal projection to filter different artifact types on long duration EEG recordings. *Comput Methods Programs Biomed* 2012;108(1): 234—49.
- [5] Boudet S, Peyrodie L, Gallois P, Vasseur C. Filtering by optimal projection and application to automatic artifact removal from EEG. *Signal Process* 2007;87(8):1978—92.
- [6] Fitzgibbon SP, Powers DMW, Pope KJ, Clark CR. Removal of EEG noise and artifact using blind source separation. *J Clin Neurophysiol Off Publ Am Electroencephalogr Soc* 2007;24(3):232—43.
- [7] Ian Daly NN. Automated artifact removal from the electroencephalogram: a comparative study. *Clin EEG Neurosci Off J EEG Clin Neurosci Soc ENCS* 2013;44(4):291—306.
- [8] Ille N, Berg P, Scherg M. Artifact correction of the ongoing EEG using spatial filters based on artifact and brain signal topographies. *J Clin Neurophysiol Off Publ Am Electroencephalogr Soc* 2002;19(2):113—24.
- [9] Jung T-P, Makeig S, Humphries C, Lee T-W, McKeown MJ, Iragui V. Removing electroencephalographic artifacts by blind source separation. *Psychophysiology* 30 2000;37(2):163—78.
- [10] LeVan P, Urrestarazu E, Gotman J. A system for automatic artifact removal in ictal scalp EEG based on independent component analysis and Bayesian classification. *Clin Neurophysiol* 2006;117(4):912—27.